

# Associated Production of Higgs and Weak Bosons, with $H \rightarrow b\bar{b}$ , at Hadron Colliders

**A. Stange and W. Marciano**

Physics Department  
Brookhaven National Laboratory  
Upton, NY 11973

**S. Willenbrock**

Department of Physics  
University of Illinois  
1110 West Green Street  
Urbana, IL 61801

## Abstract

We consider the search for the Higgs boson at a high-luminosity Fermilab Tevatron ( $\sqrt{s} = 2$  TeV), an upgraded Tevatron of energy  $\sqrt{s} = 3.5$  TeV, and the CERN Large Hadron Collider (LHC,  $\sqrt{s} = 14$  TeV), via  $WH/ZH$  production followed by  $H \rightarrow b\bar{b}$  and leptonic decay of the weak vector bosons. We show that each of these colliders can potentially observe the standard Higgs boson in the intermediate-mass range,  $80 \text{ GeV} < m_H < 120 \text{ GeV}$ . This mode complements the search for and the study of the intermediate-mass Higgs boson via  $H \rightarrow \gamma\gamma$  at the LHC. In addition, it can potentially be used to observe the lightest Higgs scalar of the minimal supersymmetric model,  $h$ , in a region of parameter space not accessible to CERN LEP II or the LHC (using  $h \rightarrow \gamma\gamma, ZZ^*$ ).

# 1 Introduction

We recently completed an analysis of the prospects for discovering the standard Higgs boson at the Fermilab Tevatron, a  $\sqrt{s} = 2$  TeV  $p\bar{p}$  collider, assuming  $1\text{ fb}^{-1}$  of integrated luminosity (which requires the Main Injector upgrade) [1]. Our motivation for undertaking that study was a desire to exploit the Tevatron to its full potential. We showed that the most promising mode is  $WH$  production, followed by  $H \rightarrow b\bar{b}$  and leptonic decay of the weak bosons [2, 3]<sup>1</sup>. We concluded that it may be possible, though challenging, to detect a Higgs boson in the mass region  $m_H = 60 - 80$  GeV using these modes (a region that will also be explored by CERN LEP II). The high luminosity which will be provided by the Main Injector ( $\mathcal{L} = 10^{32}/\text{cm}^2/\text{s}$ ) together with the ability to detect secondary vertices from  $b$  quarks with a silicon vertex detector (SVX) make the search for the Higgs boson at the Tevatron potentially viable over this limited mass range.

LEP II can search for a Higgs boson of mass up to  $80 - 85$  GeV [4]. Beyond that, the CERN Large Hadron Collider (LHC), a 14 TeV high-luminosity  $pp$  collider ( $\mathcal{L} \approx 10^{34}$ ), is planned to cover the Higgs-boson mass range from 80 GeV up to 800 GeV [5, 6]. However, the “intermediate mass” region,  $80\text{ GeV} < m_H < 120\text{ GeV}$ , is particularly difficult for hadron supercolliders. At the LHC, the search for the intermediate-mass Higgs boson relies on the rare decay mode  $H \rightarrow \gamma\gamma$ , which requires maintaining excellent photon energy and angular resolution while running at full luminosity [5, 6]. Furthermore, this signal becomes inaccessible if the branching ratio of the Higgs boson to two photons is sufficiently suppressed below the standard-model value. This can occur, for example, if the coupling of the Higgs boson to bottom quarks is enhanced with respect to the standard-model value, thereby increasing the total width of the Higgs boson, which is dominated by  $H \rightarrow b\bar{b}$  in the intermediate-mass region. Such a scenario can be realized for the light Higgs scalar (or the heavy Higgs scalar) of the minimal supersymmetric model. We therefore return to our study of the search for the Higgs boson via  $WH/ZH$ , followed by  $H \rightarrow b\bar{b}$ , to ask whether this mode could be used

---

<sup>1</sup>For a full set of references, see Ref. [1].

at future hadron colliders to search for a Higgs boson above the mass range that will be covered by LEP II. Even if an intermediate-mass Higgs boson can be detected at the LHC via  $H \rightarrow \gamma\gamma$ , it would still be valuable to observe  $WH$  production, and the decay  $H \rightarrow b\bar{b}$ , to explore the coupling of the Higgs boson to weak vector bosons and bottom quarks.

Along with the LHC, we consider two possible upgrades of the Tevatron collider at Fermilab. The first is to increase the luminosity of the machine to  $10^{33}/\text{cm}^2/\text{s}$ , and perhaps more. This could be achieved by adding several new rings of magnets, some or all in the Main Injector tunnel, to increase the intensity of the antiproton source [7, 8]. The second is to increase the energy of the machine along with the luminosity. Of the various energy upgrades which one could consider, an “energy doubler” significantly increases the physics potential of the machine, can be built on a relatively short time scale, and may be complementary to the LHC in some ways [9]. This machine would produce a large sample of top quarks and extend the search range for new physics, e. g., supersymmetry,  $Z'$  bosons, etc. The installation of a new ring of high-field magnets to replace the existing 4.4 Tesla magnets is required. The machine we consider is a 3.5 TeV (7.7 Tesla magnets)  $p\bar{p}$  collider.<sup>2</sup>

The total cross sections for the various Higgs-boson production processes at the Tevatron<sup>3</sup> and the LHC can be found in Refs. [1] and [10], respectively. We show in Fig. 1 the various cross sections at the 3.5 TeV  $p\bar{p}$  collider. The QCD corrections to  $gg \rightarrow H$  [11, 12, 13] (a factor of 2.1 in the  $\overline{MS}$  scheme with  $\mu = m_H$ ) and  $q\bar{q} \rightarrow WH/ZH$  [14] (a factor of 1.2 in the  $\overline{MS}$  scheme with  $\mu = M_{VH}$ ) are included. The  $gg \rightarrow H$  cross section is increased by a factor of about 2.5 – 4 over the corresponding Tevatron cross section for  $m_H = 60 - 200$  GeV. The  $WH/ZH$  cross section is increased by a factor of about 2 over the corresponding Tevatron cross section (see Ref. [1]).

In section 2 we reconsider our previous analysis of  $WH$  and  $ZH$  production, followed by  $H \rightarrow b\bar{b}$  and leptonic decay of the weak bosons, for the Tevatron, the  $\sqrt{s} = 3.5$  TeV  $p\bar{p}$  collider, and the LHC. We list the number of events obtained with  $10 \text{ fb}^{-1}$  of integrated

---

<sup>2</sup>Another possibility being discussed is a 4 TeV (8.8 Tesla magnets)  $p\bar{p}$  collider. The results for that machine are similar to those for the 3.5 TeV machine, as will be quantified in a later footnote.

<sup>3</sup>The name “Tevatron” will be reserved for the  $\sqrt{s} = 2$  TeV  $p\bar{p}$  collider.

luminosity; this corresponds to one “year” ( $10^7 s$ ) of running at an instantaneous luminosity of  $10^{33}/cm^2/s$ . We also consider larger integrated luminosities, with the caveat that  $b$ -tagging with high efficiency and purity, which is essential to the extraction of the signal, may prove to be difficult at higher instantaneous luminosities. With a bunch spacing of 20 ns, a luminosity of  $10^{33}/cm^2/s$  yields about 1.5 interactions per bunch crossing, which is acceptable for tagging secondary vertices with the SVX. However, with the same bunch spacing, a luminosity of  $10^{34}/cm^2/s$  yields about 15 interactions per bunch crossing. It is not known how successful  $b$ -tagging with the SVX will be in an environment with many interactions per bunch crossing.

In section 3 we consider the search for the lightest Higgs scalar,  $h$ , of the minimal supersymmetric model, which contains two Higgs doublets. There is a region of parameter space in which the light Higgs scalar (or the heavy Higgs scalar) has enhanced coupling to the  $b$  quark, suppressing the branching ratio of  $h \rightarrow \gamma\gamma$  such that it is unobservable at the LHC. We show that the mode  $Wh$ , with  $h \rightarrow b\bar{b}$ , can potentially be used to observe this Higgs boson over some of the region where  $h \rightarrow \gamma\gamma$  is unobservable. This mode is therefore complementary to the two-photon search mode for the light supersymmetric Higgs scalar at hadron colliders. In section 4 we present our conclusions.

## 2 $WH/ZH$ , with $H \rightarrow b\bar{b}$

Associated production of Higgs and weak vector bosons, with  $H \rightarrow b\bar{b}$ , was considered in detail at the Tevatron in our previous study [1]. The analysis here closely follows that work, and we refer the reader to that paper for additional details. The weak bosons are detected via their leptonic decays ( $W \rightarrow \ell\nu, Z \rightarrow \ell\ell$ ). The cuts made to simulate the acceptance of the detector are listed in Table 1. The jet energy resolution is taken to be  $\Delta E_j/E_j = 0.80/\sqrt{E_j} \oplus 0.05$ , which corresponds to a two-jet invariant-mass resolution of about  $\Delta M_{jj}/M_{jj} = 0.80/\sqrt{M_{jj}} \oplus 0.03$  (added in quadrature).<sup>4</sup> We integrate the background

---

<sup>4</sup>The two-jet invariant-mass resolution may be degraded somewhat due to semileptonic  $b$  decays, which occur in 40% of the events.

over an invariant-mass bin of  $\pm 2\Delta M_{jj}$ ; for  $M_{jj} = 100$  GeV, this amounts to a bin width of 34 GeV. A change from our previous analysis is that we reduce the  $p_T$  threshold for observing charged leptons to  $p_T > 10$  GeV (although we continue to trigger on leptons of  $p_T > 20$  GeV). This is important for rejecting the top-quark background to the  $WH$  signal. We also extend the coverage for jets out to a rapidity of 4, for the same reason. We will comment on the effect of reducing the jet coverage to a rapidity of 2.5 at the Fermilab machines.

Table 1: Acceptance cuts used to simulate the detector. The  $p_{T\ell}$  threshold is greater for charged leptons which are used as triggers (in parentheses).

$$\begin{array}{ll}
|\eta_b| < 2 & p_{Tb} > 15 \text{ GeV} \\
|\eta_\ell| < 2.5 & p_{T\ell} > 10 \text{ GeV (20 GeV)} \\
|\eta_j| < 4 & p_{Tj} > 15 \text{ GeV} \\
|\Delta R_{b\bar{b}}| > 0.7 & |\Delta R_{b\ell}| > 0.7 \\
\not{p}_T > 20 \text{ GeV} & (\text{for } W \rightarrow \ell\bar{\nu})
\end{array}$$

The cross sections for the signals and backgrounds at the Tevatron, the 3.5 TeV  $p\bar{p}$  collider, and the LHC, including all branching ratios and acceptances, are shown in Figs. 2, 3, and 4, respectively. The  $WH/ZH$  cross sections at the 3.5 TeV collider and the LHC are increased by factors of about 2 and 4, respectively, after acceptance cuts, over the corresponding cross sections at the Tevatron. The dominant irreducible backgrounds are  $Wb\bar{b}/Zb\bar{b}$  and, for  $m_H$  near  $M_Z$ ,  $WZ/ZZ$  with  $Z \rightarrow b\bar{b}$ . The dominant reducible background is  $Wjj/Zjj$  (not shown in the figures).<sup>5</sup> In our previous study, we demanded that at least one jet be identified as a  $b$  jet to reduce this background; it nevertheless remained the dominant background, assuming a 1% misidentification of a jet as a  $b$  jet. When one considers higher luminosity, one obtains enough  $WH/ZH$  signal events that it becomes advantageous to demand that *both* jets be identified as  $b$  jets. This greatly reduces the  $Wjj/Zjj$  background. At the Fermilab colliders, this background is significantly less than the irreducible  $Wb\bar{b}/Zb\bar{b}$  background, while at the LHC the  $Wjj$  background is comparable to the  $Wb\bar{b}$  background, and  $Zjj$  is negligible compared with  $Zb\bar{b}$ . The  $Wjj/Zjj$  background is relatively larger

---

<sup>5</sup>The  $Wjj$  and  $Zjj$  backgrounds were calculated using the code developed in Ref. [15].

at the LHC because it is initiated mostly by gluon-quark collisions, while the signal arises from quark-antiquark annihilation. Similarly, the  $Zb\bar{b}$  background at the LHC is initiated by gluon-gluon collisions, which accounts for its relatively large size. Assuming an efficiency  $\epsilon_b = 0.3$  for tagging a  $b$  jet within the fiducial volume of the SVX and with  $p_T > 15$  GeV, we use  $\epsilon_b^2 = 0.09$  as an estimate of the efficiency for a double  $b$  tag.

Another reducible background to the  $Wb\bar{b}$  signal is from  $t\bar{t}$  production, followed by  $t\bar{t} \rightarrow b\bar{b}W^+W^-$  with one  $W$  missed. Reduction of this background requires coverage of leptons to small  $p_T$  and jets to high rapidity, to reduce the likelihood of missing a  $W$  boson. We reject events with a hadronic decay of the additional  $W$  boson if a jet from the  $W$  decay with  $p_T > 30$  GeV, or two jets with  $p_T > 15$  GeV (and invariant mass near  $M_W$ ), are observed. We calculate that the signal is accompanied by jets exceeding these cuts only about 10% of the time at the Fermilab machines, and 30% of the time at the LHC [14].<sup>6</sup> We also impose the requirement that the transverse mass of the trigger charged lepton plus the missing  $p_T$  be less than  $M_W$ , which is almost always true for the signal. The resulting cross sections for  $m_t = 170$  GeV (the approximate central value from precision electroweak experiments [16]) are shown in Figs. 2 – 4.<sup>7</sup> At the Fermilab colliders, the  $t\bar{t}$  background to the  $WH$  signal never exceeds the  $Wb\bar{b}$  background, and is significant only for  $m_H > 100$  GeV at the 3.5 TeV collider. At the LHC,  $t\bar{t}$  is the biggest background to the  $WH$  signal for  $m_H > 80$  GeV. The  $t\bar{t}$  background at the LHC is relatively large because it is initiated by gluon-gluon collisions, while the signal arises from quark-antiquark annihilation. This background increases at the Fermilab colliders and the LHC by factors of roughly 2 and 1.7, respectively, for every 20 GeV decrease in the top-quark mass. At the Fermilab colliders, about 60% of the remaining  $t\bar{t}$  background events are from the leptonic decay of the missed  $W$  boson, and 40% from the hadronic decay, for  $m_H = 100$  GeV; the ratio drops to 50/50 for  $m_H = 140$  GeV. Decreasing the jet coverage to a rapidity of 2.5 increases the hadronic contribution by about 50%, thus

---

<sup>6</sup>We do not reduce the signal to account for the rejection of events due to jet radiation. The backgrounds will also have jet radiation, and it is beyond the scope of this work to include these effects.

<sup>7</sup>The  $t\bar{t}$  background in Fig. 2(a) is reduced from our previous study, Fig. 3(a) of Ref. [1], due to the increased coverage for leptons and jets assumed of the detector.

increasing the net  $t\bar{t}$  background by only about 20 – 25%. At the LHC, the ratio of leptonic to hadronic missed- $W$  events is about 70/30 at  $m_H = 100$  GeV, decreasing to about 67/33 at  $m_H = 140$  GeV.

There are other sources of top quarks at hadron colliders which can contribute to the  $WH/ZH$  background. Single-top-quark production via  $W$ -gluon fusion,  $Wg \rightarrow t\bar{b}$ , in which the “initial” (virtual)  $W$  boson is radiated from an incoming quark, yields a  $Wb\bar{b} + q$  final state after the top quark decays [17].<sup>8</sup> We suppress this background by rejecting events in which the jet formed from the outgoing quark has rapidity less than 4 and  $p_T > 30$  GeV. The resulting background is shown in Figs. 2 – 4; it is comparable to the  $t\bar{t}$  background. The  $Wg \rightarrow t\bar{b}$  background increases at the Fermilab colliders and the LHC by factors of roughly 1.4 and 1.2, respectively, for every 20 GeV decrease in the top-quark mass.

Single-top-quark production can also occur via the weak process  $q\bar{q} \rightarrow t\bar{b}$ , which again yields a  $Wb\bar{b}$  final state after the top quark decays. This is an irreducible background, since there are no additional particles in the final state. This background is also shown in Figs. 2 – 4; it is comparable to the other top-quark backgrounds at the Fermilab machines, but relatively much smaller at the LHC. It increases at the Fermilab colliders and the LHC by factors of roughly 1.7 and 1.5, respectively, for every 20 GeV decrease in the top-quark mass.

We list in Table 2 the number of signal and background events per 10  $fb^{-1}$  of integrated luminosity, with a double  $b$  tag, at the Tevatron, the 3.5 TeV  $p\bar{p}$  collider<sup>9</sup>, and the LHC, for a variety of Higgs-boson masses. The statistical significance of the signal,  $S/\sqrt{B}$ , is listed in the last column for the  $WH/ZH$  processes. If we define discovery of the  $WH$  signal by the criterion of a  $5\sigma$  significance, then with 30  $fb^{-1}$  of integrated luminosity the reach of the Tevatron is about  $m_H = 95$  GeV, the reach of the 3.5 TeV  $p\bar{p}$  collider about 100 GeV, and the reach of the LHC also about 100 GeV. The largest background at the Fermilab machines is  $Wb\bar{b}$ , while at the LHC it is  $t\bar{t}$  and  $Wg \rightarrow t\bar{b}$ . The  $t\bar{t}$  cross sections in Figs. 2 – 4 represent a reduction of the  $t\bar{t}$  cross section, before rejecting the additional  $W$  boson but with

---

<sup>8</sup>We thank Chris Hill for bringing the single-top-quark backgrounds to our attention.

<sup>9</sup>At a 4 TeV  $p\bar{p}$  collider, the  $WH/ZH$  signal and the backgrounds  $Wb\bar{b}/Zb\bar{b}$  and  $WZ/ZZ$  increase by about 15% from the 3.5 TeV machine, increasing the significance of the signal by roughly 7%.

acceptance cuts, by a factor of about  $1/35$  at the Fermilab machines, and about  $1/25$  at the LHC. If the rejection could be improved at the LHC, it would increase the significance of the signal. The corresponding rejection factor for the extra jet in the  $Wg \rightarrow t\bar{b}$  process is only a factor of about  $1/3$ . If the top-quark mass proves to be closer to 190 GeV, the significance of the LHC signal would increase by about 10%. If the misidentification probability of a light-quark jet as a  $b$  jet is increased from 1% to 2%, the  $Wjj$  background quadruples, but since it is not the largest background at any of the machines, the statistical significance of the  $WH$  signal drops by only about 15%.

If integrated luminosities in excess of  $30\text{ fb}^{-1}$  can be achieved, one can observe Higgs bosons of greater mass. With  $100\text{ fb}^{-1}$ , the reach of the Tevatron is about 120 GeV, the 3.5 TeV  $p\bar{p}$  collider about 125 GeV, and the LHC about 120 GeV. Thus each machine is potentially capable of covering the intermediate-mass region. However, one must keep in mind the caveat in the Introduction regarding  $b$  tagging at high luminosity.

The significance of the  $ZH$  signal is much less than that of the  $WH$  signal due to the small branching ratio of the  $Z$  boson to charged leptons.<sup>10</sup> If the decay of the  $Z$  boson to neutrinos could be used as well, it would increase the significance of the signal by a factor of roughly 2.4, making it comparable to that of the  $WH$  signal. However, the  $ZH$  signal with  $Z \rightarrow \nu\bar{\nu}$ ,  $H \rightarrow b\bar{b}$ , has no simple trigger, and suffers from potentially large backgrounds from the QCD production of  $b\bar{b}j$  where the jet is either mismeasured or carries away significant  $p_T$  outside of the rapidity coverage of the detector.<sup>11</sup> It remains to be shown whether a minimum missing  $p_T$  threshold exists which reduces the background while maintaining a significant fraction of the signal. The observation of a signal in the  $ZH$  channel would be valuable to confirm a signal in the  $WH$  channel.

The  $WZ/ZZ$  background can be normalized by using the purely leptonic decay mode. However, the Higgs peak at  $m_H = 90$  GeV is about 75% of the  $Z$  peak (for the  $WH$  signal). Thus, if the Higgs-boson mass happens to lie near the  $Z$  mass, it will be difficult to convince

---

<sup>10</sup>In our previous analysis at the Tevatron, Ref. [1], we included the decay of the  $Z$  boson to neutrinos. We do not include this mode in this analysis because of the ensuing reasons in the text.

<sup>11</sup>We thank J. Gunion and T. Han for this observation.



oneself that the observed peak in the  $b\bar{b}$  invariant-mass spectrum is really the sum of the Higgs peak and the  $Z$  peak, and not just the  $Z$  peak with an underestimate of the  $b$ -tagging efficiency. If the Higgs mass is sufficiently different from the  $Z$  mass, one should observe both the Higgs and the  $Z$  peaks. Better dijet invariant-mass resolution would be helpful to separate the peaks, as well as to increase the statistical significance of the signals.

If a Higgs boson is discovered via  $WH$ , with  $H \rightarrow b\bar{b}$ , the determination of the Higgs-boson mass will be limited by the  $b\bar{b}$  invariant-mass resolution. However, a precise measurement of the Higgs-boson mass can be made via its decay to two photons, if this mode proves to be observable.

### 3 The light Higgs scalar of the minimal supersymmetric model

In a two-Higgs-doublet model, the couplings of one or more of the physical Higgs bosons (two neutral scalars,  $h$  and  $H$ ; a neutral pseudoscalar,  $A$ ; and a charged scalar,  $H^\pm$ ) to a given fermion are generally enhanced [18]. The Higgs sector of the minimal supersymmetric model is a two-Higgs-doublet model which is determined (at tree level) by two parameters, conventionally chosen to be the ratio of the Higgs-field vacuum-expectation values,  $v_2/v_1 \equiv \tan \beta$ , and the mass of the neutral pseudoscalar,  $m_A$  [19]. Most models employ radiative electroweak symmetry breaking [20], which requires  $\tan \beta > 1$ , ranging up to  $\tan \beta \approx m_t/m_b$ , which one obtains in the simplest  $SO(10)$  grand-unified models [21, 22]. For  $\tan \beta > 1$  the coupling of all the Higgs bosons to bottom quarks is enhanced over the standard-model coupling.

There is an upper bound on the mass of the lightest Higgs scalar,  $h$ , which depends on the top-quark mass and the top-squark masses, as well as on other parameters which we ignore for this discussion [23]. This upper bound is attained for large  $\tan \beta$ , and is given by

$$m_h^2 < M_Z^2 + \frac{3G_F}{\pi^2\sqrt{2}}m_t^4 \ln \frac{m_{\tilde{t}_1}m_{\tilde{t}_2}}{m_t^2} \quad (1)$$

where  $m_{\tilde{t}_{1,2}}$  are the masses of the top squarks. For  $m_{\tilde{t}_{1,2}} = 500$  GeV, the upper bound is

$m_h < 107, 113, 121$  GeV for  $m_t = 150, 170, 190$  GeV, respectively. For  $m_{\tilde{t}_{1,2}} = 1$  TeV, the upper bound is  $m_h < 115, 125, 138$  GeV, respectively.

For a given value of  $\tan\beta$ , the upper limit on  $m_h$  is approached as  $m_A \rightarrow \infty$ , and the coupling of the  $h$  to bottom quarks (and to all other standard-model particles) becomes of standard-model strength. This particle can be detected at the LHC via  $h \rightarrow \gamma\gamma$  or  $h \rightarrow ZZ^{(*)} \rightarrow l^+l^-l^+l^-$ . However, for  $m_A \sim 100 - 200$  GeV and  $\tan\beta > 2$ , the  $h$  is too heavy to be produced at LEP II, and its branching ratio to two photons is too suppressed to be detected at the LHC. This leads to the well-known “hole” in the  $m_A, \tan\beta$  plane in which the  $h$  (as well as the other Higgs particles,  $H$ ,  $A$ , and perhaps also  $H^\pm$ , depending on the top-quark mass) cannot be detected by either LEP II or LHC (using the above decay modes) [5, 6, 24, 25, 26, 27].

The hole in the  $m_A, \tan\beta$  plane is due to the enhanced coupling of  $h$  to bottom quarks, which suppresses the branching ratio of  $h \rightarrow \gamma\gamma$ . It is therefore a natural place to make use of the process  $Wh$ , with  $h \rightarrow b\bar{b}$ . The Tevatron, the 3.5 TeV  $p\bar{p}$  collider, and the LHC can potentially detect  $Wh$ , with  $h \rightarrow b\bar{b}$ , as long as  $h$  is not so heavy that its branching ratio to  $b\bar{b}$  is suppressed by its decay to  $WW^{(*)}$ . For large  $\tan\beta$ , the coupling of  $h$  to bottom quarks is sufficiently enhanced that this branching ratio is close to its maximum value of 92% all the way up to the real  $WW$  threshold. Because of this, larger Higgs-boson masses can be accessed in the minimal supersymmetric model than in the standard model, where the branching ratio to  $b\bar{b}$  begins to fall off at  $m_H \approx 110$  GeV (see Fig. 2 in Ref. [1]).

We show in Figs. 5, 6, and 7 the discovery reach for the lightest supersymmetric Higgs scalar via  $Wh$ , with  $h \rightarrow b\bar{b}$ , at the Tevatron, the 3.5 TeV  $p\bar{p}$  collider, and the LHC, respectively, in the  $m_A, \tan\beta$  plane, assuming a.)  $m_{\tilde{t}_{1,2}} = 500$  GeV and b.)  $m_{\tilde{t}_{1,2}} = 1$  TeV. The contours indicate the number of  $fb^{-1}$  of integrated luminosity needed to yield a  $5\sigma$  signal (for  $m_h > 50$  GeV, the approximate lower bound from LEP I [28]). To guide the eye, the regions corresponding to 50  $fb^{-1}$  or less have been shaded. The upper right-hand corner of each plot corresponds to  $h$  at the maximum value of its mass and with standard-model couplings, so it is as difficult to detect as the standard Higgs boson of the same mass. As the

top-squark masses decrease, the upper bound on  $m_h$  decreases, and more of the  $m_A, \tan \beta$  plane is covered for a given amount of integrated luminosity. At all three machines,  $h$  can be detected with  $30 \text{ fb}^{-1}$  only in the region  $\tan \beta < 4$ . With  $50 \text{ fb}^{-1}$  of integrated luminosity, the hole where the  $h$  is not accessible to LEP II and the LHC (via  $h \rightarrow \gamma\gamma, ZZ^*$ ) is almost entirely filled at the 3.5 TeV machine for  $m_{\tilde{t}_{1,2}} = 500 \text{ GeV}$  (Fig. 6(a)) and is partially filled at the 3.5 TeV machine for  $m_{\tilde{t}_{1,2}} = 1 \text{ TeV}$  (Fig. 6(b)) and the LHC for  $m_{\tilde{t}_{1,2}} = 500 \text{ GeV}$  (Fig. 7(a)). With  $100 \text{ fb}^{-1}$ , almost all of the hole is filled at all three machines. This demonstrates that the coverage of the "hole" region is sensitive to small changes in the analysis. The upper bound on  $m_h$  increases as the top-quark mass increases, but this is largely compensated by the decrease in the top-quark backgrounds, such that the coverage of the  $m_A, \tan \beta$  plane is not very sensitive to the top-quark mass. If decays of  $h$  to pairs of supersymmetric particles are kinematically available, they may decrease the branching ratio of  $h \rightarrow b\bar{b}$ , although for large  $\tan \beta$  this decay may still dominate.

It may also be possible to observe the heavy Higgs scalar,  $H$ , of the minimal supersymmetric model via  $WH$ , with  $H \rightarrow b\bar{b}$ , if  $H$  is relatively light. For a fixed value of  $\tan \beta$ , the heavy Higgs scalar approaches its lower bound, which is the same as the upper bound on the mass of the light Higgs scalar, Eq. 1, as  $m_A \rightarrow 0$ . For large  $\tan \beta$ , there is a region of parameter space in which  $H$  is near its lower bound,  $h$  is heavier than 50 GeV, the coupling of  $H$  to weak vector bosons is almost of standard-model strength, and its coupling to bottom quarks is at least of standard-model strength. This region lies roughly between  $m_A = 50$  and 100 GeV for large  $\tan \beta$ , depending on the top-quark mass and the top-squark masses.

## 4 Conclusions

The intermediate-mass Higgs boson,  $80 \text{ GeV} < m_H < 120 \text{ GeV}$ , is elusive. It is too heavy to be produced at LEP II, and can be discovered at the LHC using the rare two-photon decay mode only if excellent photon energy and angular resolution can be maintained while running at full luminosity ( $\mathcal{L} \approx 10^{34}/\text{cm}^2/\text{s}$ ). We have shown that Higgs-boson production

in association with a weak vector boson, followed by  $H \rightarrow b\bar{b}$  and leptonic decay of the weak vector boson, can potentially be used to observe the standard Higgs boson in the intermediate-mass range at future hadron colliders. The machines we considered are the Fermilab Tevatron ( $\sqrt{s} = 2$  TeV) with high luminosity ( $\mathcal{L} \geq 10^{33}/\text{cm}^2/\text{s}$ ), an upgraded Tevatron of energy  $\sqrt{s} = 3.5$  TeV with high luminosity, and the LHC ( $\sqrt{s} = 14$  TeV). With  $30 \text{ fb}^{-1}$  of integrated luminosity, a  $5\sigma$  signal is possible in the  $WH$  channel for a Higgs boson of mass up to about 95 GeV at the Tevatron, about 100 GeV at the 3.5 TeV  $p\bar{p}$  collider, and also about 100 GeV at the LHC. With  $100 \text{ fb}^{-1}$  of integrated luminosity, the reach of the Tevatron, the 3.5 TeV  $p\bar{p}$  collider, and the LHC is about 120, 125, and 120 GeV, respectively. However, to gather this amount of integrated luminosity would require  $b$ -tagging in an environment with many interactions per bunch crossing, which may prove to be difficult. We conclude that each of these machines can potentially cover the intermediate-mass region.

If the coupling of the Higgs boson to bottom quarks is enhanced, the decay of the intermediate-mass Higgs boson to two photons can be suppressed such that it is unobservable at the LHC. This can occur for the light Higgs scalar,  $h$ , of the minimal supersymmetric model, whose mass lies within or below the intermediate-mass region if the top quark and the top squarks are not too heavy. The enhanced coupling of  $h$  to bottom quarks increases the mass at which the branching ratio of  $h \rightarrow b\bar{b}$  begins to fall off due to the competition from  $h \rightarrow WW^{(*)}$ . We showed that the mode  $Wh$ , with  $h \rightarrow b\bar{b}$ , can potentially cover part of the parameter space of the minimal supersymmetric model not accessible to LEP II or the LHC (using  $h \rightarrow \gamma\gamma, ZZ^*$ ). It is also possible that the heavy Higgs scalar of the minimal supersymmetric model,  $H$ , can be observed via  $WH$  production over part of the parameter space.

We hope that this paper will revitalize interest in associated production of Higgs and weak vector bosons, with  $H \rightarrow b\bar{b}$ , at future hadron colliders. We encourage the detector collaborations at the Tevatron and the LHC to undertake a deeper study of the potential usefulness of this mode.

## 5 Acknowledgements

We are grateful for conversations with M. Albrow, D. Amidei, J. Butler, S. Dawson, K. Einsweiler, D. Errede, S. Errede, D. Finley, B. Foster, H. Gordon, J. Gunion, T. Han, C. Hill, I. Hinchliffe, L. Holloway, R. Kauffman, T. LeCompte, T. Liss, F. Paige, S. Protopopescu, X. Tata, and H. Weerts. This work was supported under contract no. DE-AC02-76CH00016 with the U.S. Department of Energy.

## References

- [1] A. Stange, W. Marciano, and S. Willenbrock, *Phys. Rev. D* **49**, 1354 (1994).
- [2] S. Glashow, D. Nanopoulos, and A. Yildiz, *Phys. Rev. D* **18**, 1724 (1978).
- [3] J. Gunion, P. Kalyniak, M. Soldate, and P. Galison, *Phys. Rev. Lett.* **54**, 1226 (1985); *Phys. Rev. D* **34**, 101 (1986).
- [4] S. L. Wu *et al.*, in *Proceedings of the ECFA Workshop on LEP 200*, Aachen, 1986, eds. A. Böhm and W. Hoogland, CERN 87-08, Vol. II, p. 312.
- [5] ATLAS Letter of Intent, CERN/LHCC/92-4 (1992).
- [6] CMS Letter of Intent, CERN/LHCC/92-3 (1992).
- [7] S. Holmes, G. Dugan, and S. Peggs, in *Research Directions for the Decade*, Proceedings of the 1990 Summer Study on High Energy Physics, Snowmass, Colorado, 1990, edited by E. Berger (World Scientific, Singapore, 1992), p. 674.
- [8] G. Jackson, private communication.
- [9] *Physics at Fermilab in the 1990's*, Breckenridge, CO, eds. D. Green and H. Lubatti (World Scientific, Singapore, 1990).
- [10] Z. Kunszt and W. J. Stirling, in *Proceedings of the ECFA Large Hadron Collider Workshop*, Aachen, 1990, eds. G. Jarlskog and D. Rein, CERN 90-10, Vol. II, p. 428.

- [11] S. Dawson, Nucl. Phys. **B359**, 283 (1991); A. Djouadi, M. Spira, and P. Zerwas, Phys. Lett. **264B**, 440 (1991).
- [12] D. Graudenz, M. Spira, and P. Zerwas, Phys. Rev. Lett. **70**, 1372 (1993).
- [13] S. Dawson and R. Kauffman, private communication; BNL-DK-1 (1993).
- [14] T. Han and S. Willenbrock, Phys. Lett. **273B**, 167 (1990); J. Ohnemus and W. J. Stirling, Phys. Rev. D **47**, 2722 (1993); H. Baer, B. Bailey, and J. Owens, Phys. Rev. D **47**, 2730 (1993).
- [15] V. Barger, T. Han, J. Ohnemus, and D. Zeppenfeld, Phys. Rev. Lett. **62**, 1971 (1989); Phys. Rev. D **40**, 2888 (1989); D **41**, 1715(E) (1990).
- [16] ALEPH, DELPHI, L3, OPAL, and the LEP Electroweak Working Group, CERN-PPE-93-157 (1993).
- [17] S. Willenbrock and D. Dicus, Phys. Rev. D **34**, 155 (1986); C.-P. Yuan, Phys. Rev. D **41**, 42 (1990); R. K. Ellis and S. Parke, Phys. Rev. D **46**, 3785 (1992).
- [18] H. Haber, G. Kane, and T. Sterling, Nucl. Phys. **B161**, 493 (1979).
- [19] For a review, see J. Gunion, H. Haber, G. Kane, and S. Dawson, *The Higgs Hunter's Guide* (Addison-Wesley, New York, 1990).
- [20] For a review, see L. Ibáñez and G. Ross, in *Perspectives on Higgs Physics*, edited by G. Kane (World Scientific, Singapore, 1993), p. 229.
- [21] B. Ananthanarayan, G. Lazarides, and Q. Shafi, Phys. Rev. D **44**, 1613 (1991)
- [22] H. Arason, D. Castaño, B. Kesathelyi, S. Mikaelian, E. Piard, P. Ramond, and B. Wright, Phys. Rev. Lett. **67**, 2933 (1991).
- [23] For a review, see H. Haber, in *The Decay Properties of SUSY Particles*, Proceedings of the 23<sup>rd</sup> Workshop of the INFN Eloisatron Project, Erice, Italy, 1992 (to be published), SCIPP-93/06.

- [24] Z. Kunszt and F. Zwirner, Nucl. Phys. **B385**, 3 (1992).
- [25] H. Baer, M. Bisset, C. Kao, and X. Tata, Phys. Rev. D **46**, 1067 (1992); H. Baer, M. Bisset, D. Dicus, C. Kao, and X. Tata, Phys. Rev. D **47**, 1062 (1993).
- [26] J. Gunion and L. Orr, Phys. Rev. D **46**, 2052 (1992).
- [27] V. Barger, K. Cheung, R. Phillips, and A. Stange, Phys. Rev. D **46**, 4914 (1992).
- [28] ALEPH Collaboration, Phys. Rep. **216**, 253 (1992).
- [29] P. Harriman, A. Martin, R. Roberts, and W. J. Stirling, Phys. Rev. D **42**, 798 (1990).

Table 2: Number of signal and background events at the Tevatron, the  $\sqrt{s} = 3.5$  TeV  $p\bar{p}$  collider, and the LHC, per  $10 \text{ fb}^{-1}$  of integrated luminosity, for production of the Higgs boson in association with a weak vector boson, followed by  $H \rightarrow b\bar{b}$  and  $W \rightarrow \ell\bar{\nu}$ ,  $Z \rightarrow \ell\bar{\ell}$ . The statistical significance of the signal,  $S/\sqrt{B}$ , is listed in the last column for the  $WH/ZH$  processes. The cuts made to simulate the acceptance of the detector are listed in Table 1. We assume a 30% efficiency for detecting a secondary vertex per  $b$  jet, within the rapidity coverage of the vertex detector and with  $p_{Tb} > 15$  GeV. We demand that both  $b$  jets be identified. We also assume a 1% misidentification of light-quark and gluon jets as a  $b$  jet. The  $t\bar{t} \rightarrow b\bar{b}W^+W^-$  background to the  $WH$  signal is reduced by rejecting events with an additional  $W$  boson, which is identified either via a charged lepton, a jet of  $p_T > 30$  GeV, or two jets with  $p_T > 15$  GeV. The  $Wg \rightarrow t\bar{b}$  background is reduced by rejecting events with an additional jet of  $p_T > 30$  GeV.

$m_H$ (GeV)	Tevatron    2 TeV $p\bar{p}$							
	$WH/ZH$	$Wb\bar{b}/Zb\bar{b}$	$WZ/ZZ$	$Wjj/Zjj$	$t\bar{t}$	$Wg \rightarrow t\bar{b}$	$q\bar{q} \rightarrow t\bar{b}$	Signif.
60	90/14	108/16	-	17/2	3/-	4.7/-	11/-	7.5/3.4
80	50/8.5	70/14	30/7.4	13/1.6	3/-	5.9/-	16/-	4.3/1.7
90	37/6.5	59/12	45/11	11/1.4	4/-	5.8/-	18/-	3.1/1.3
100	27/4.9	45/9.4	37/9	9/1.3	4/-	5.4/-	20/-	2.5/1.1
120	14/2.5	31/6.7	3/0.72	6.5/0.9	5/-	4.4/-	21/-	1.7/0.87
140	5.4/0.88	20/4.5	-	4.5/0.72	5/-	3.2/-	20/-	0.74/0.38
3.5 TeV $p\bar{p}$								
60	138/23	183/48	-	43/5.4	11/-	21/-	19/-	8.3/3.1
80	81/14	121/41	59/13	33/5	16/-	26/-	29/-	4.8/1.8
90	61/11	99/37	89/20	30/4.7	18/-	26/-	33/-	3.6/1.4
100	47/8.6	82/30	73/17	26/4.1	19/-	25/-	36/-	2.9/1.2
120	26/4.7	58/23	6/1.3	19/3.4	22/-	20/-	40/-	2.0/0.89
140	10/1.8	43/17	-	15/2.7	24/-	16/-	40/-	0.83/0.41
LHC    14 TeV $pp$								
60	281/58	394/409	-	186/44	291/-	286/-	42/-	8.5/2.7
80	170/36	285/395	119/46	169/49	407/-	392/-	62/-	4.6/1.6
90	132/28	237/369	178/68	159/47	448/-	376/-	70/-	3.4/1.3
100	104/22	199/349	146/56	142/44	481/-	364/-	77/-	2.8/1
120	60/13	145/276	12/4.5	115/38	529/-	312/-	84/-	1.7/0.68
140	24/4.9	110/220	-	94/31	552/-	257/-	83/-	0.72/0.31



## 6 Figure Captions

Fig. 1 - Cross sections for various Higgs-boson production processes at a  $\sqrt{s} = 3.5$  TeV  $p\bar{p}$  collider, versus the Higgs-boson mass. The HMRSB parton distribution functions [29] are used for all calculations. The top-quark mass is taken to be 170 GeV.

Fig. 2 - Cross sections and backgrounds at the Tevatron ( $\sqrt{s} = 2$  TeV) for a.)  $WH$  and b.)  $ZH$  production, followed by  $H \rightarrow b\bar{b}$  and  $W \rightarrow \ell\bar{\nu}$ ,  $Z \rightarrow \ell\bar{\ell}$ , versus the Higgs-boson mass. The cuts made to simulate the acceptance of the detector are listed in Table 1. The backgrounds are from  $Wb\bar{b}$  and  $Zb\bar{b}$ ;  $WZ$  and  $ZZ$  followed by  $Z \rightarrow b\bar{b}$ ;  $t\bar{t} \rightarrow W^+W^-b\bar{b}$  with one  $W$  missed;  $Wg \rightarrow t\bar{b} \rightarrow Wb\bar{b}$ ; and  $q\bar{q} \rightarrow t\bar{b} \rightarrow Wb\bar{b}$  (the top-quark backgrounds for the  $WH$  signal only). The top-quark mass is taken to be 170 GeV.

Fig. 3 - Same as Fig. 2, but for the  $\sqrt{s} = 3.5$  TeV  $p\bar{p}$  collider.

Fig. 4 - Same as Fig. 2, but for the LHC ( $\sqrt{s} = 14$  TeV  $pp$ ).

Fig. 5 - Contour plots in the  $m_A, \tan\beta$  plane of the number of  $fb^{-1}$  of integrated luminosity required to observe a  $5\sigma$  signal for the light Higgs scalar,  $h$ , of the minimal supersymmetric model via the process  $Wh$ , with  $h \rightarrow b\bar{b}$ , at the Tevatron ( $\sqrt{s} = 2$  TeV). For a given value of the pseudoscalar Higgs mass,  $m_A$ , and the ratio of the Higgs-field vacuum-expectation values,  $v_2/v_1 \equiv \tan\beta$ , the mass of  $h$  depends on the top-quark mass and the top-squark masses. The figures are for a.)  $m_{\tilde{t}_{1,2}} = 500$  GeV and b.)  $m_{\tilde{t}_{1,2}} = 1$  TeV. The top-quark mass is taken to be 170 GeV; however, the figures are insensitive to the top-quark mass, as explained in the text. The regions of  $50 fb^{-1}$  or less are shaded to guide the eye.

Fig. 6 - Same as Fig. 5, but for the  $\sqrt{s} = 3.5$  TeV  $p\bar{p}$  collider.

Fig. 7 - Same as Fig. 5, but for the LHC ( $\sqrt{s} = 14$  TeV).

This figure "fig1-1.png" is available in "png" format from:

<http://arxiv.org/ps/hep-ph/9404247v2>

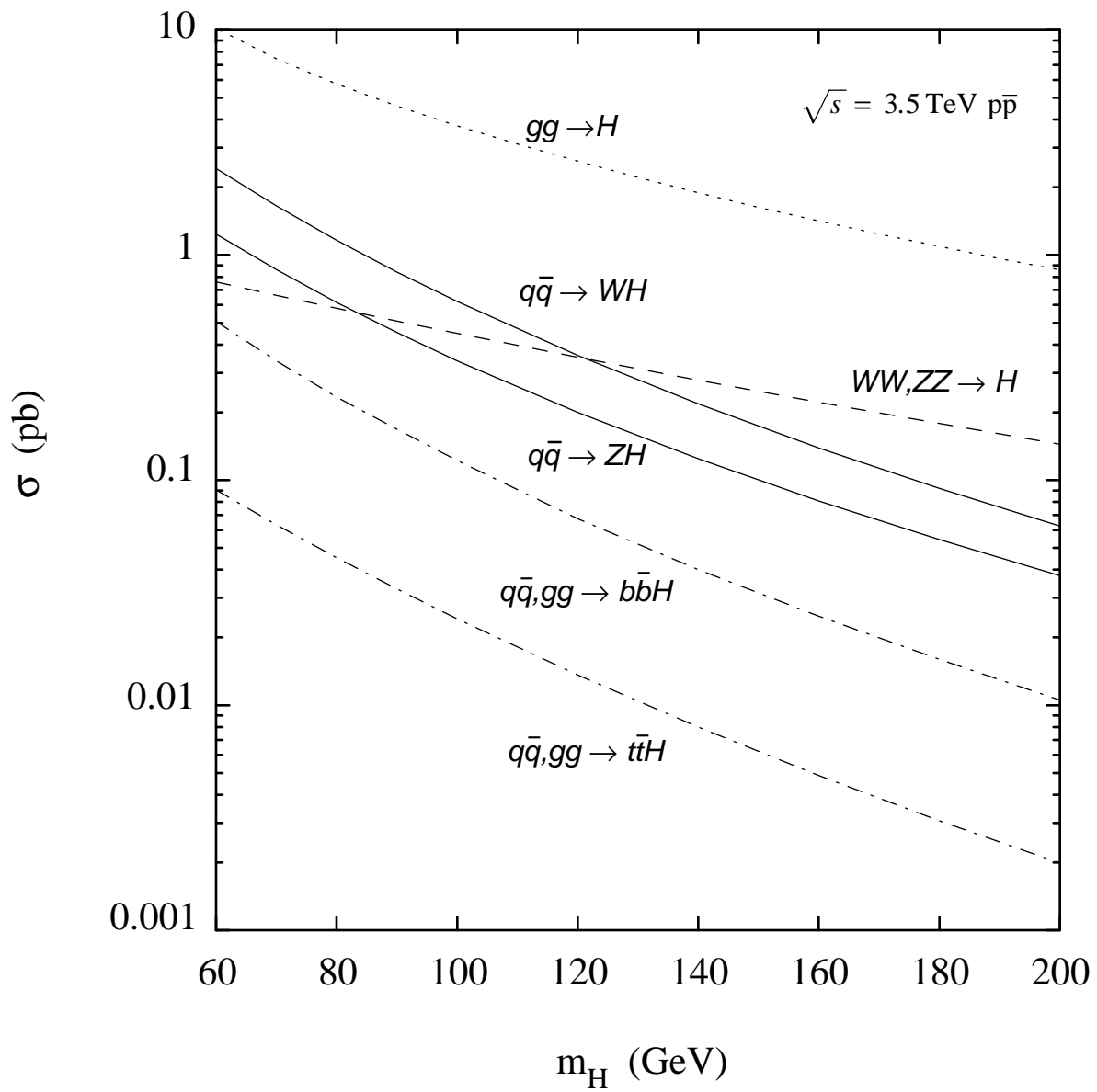


Figure 1

This figure "fig1-2.png" is available in "png" format from:

<http://arxiv.org/ps/hep-ph/9404247v2>

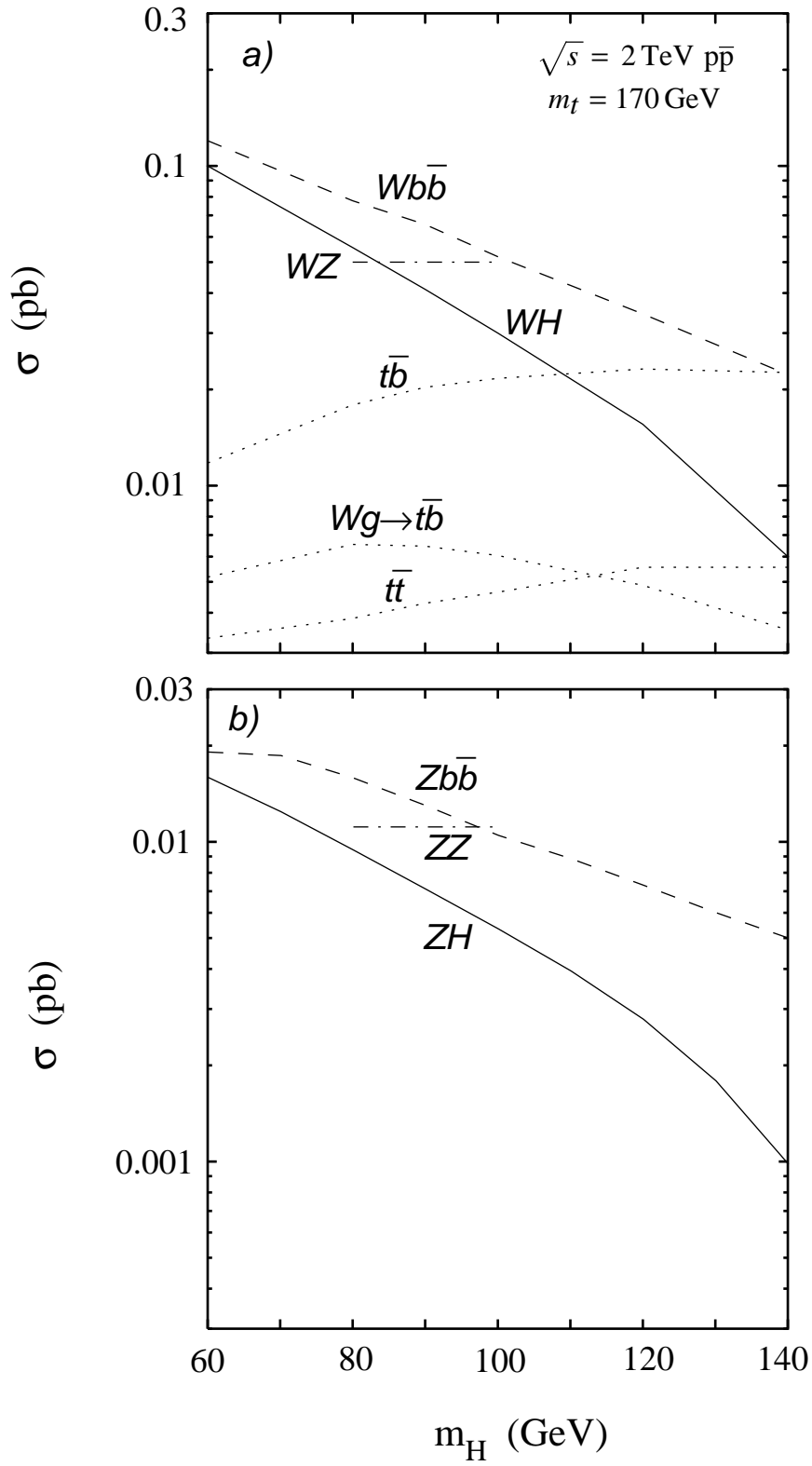


Figure 2

This figure "fig1-3.png" is available in "png" format from:

<http://arxiv.org/ps/hep-ph/9404247v2>

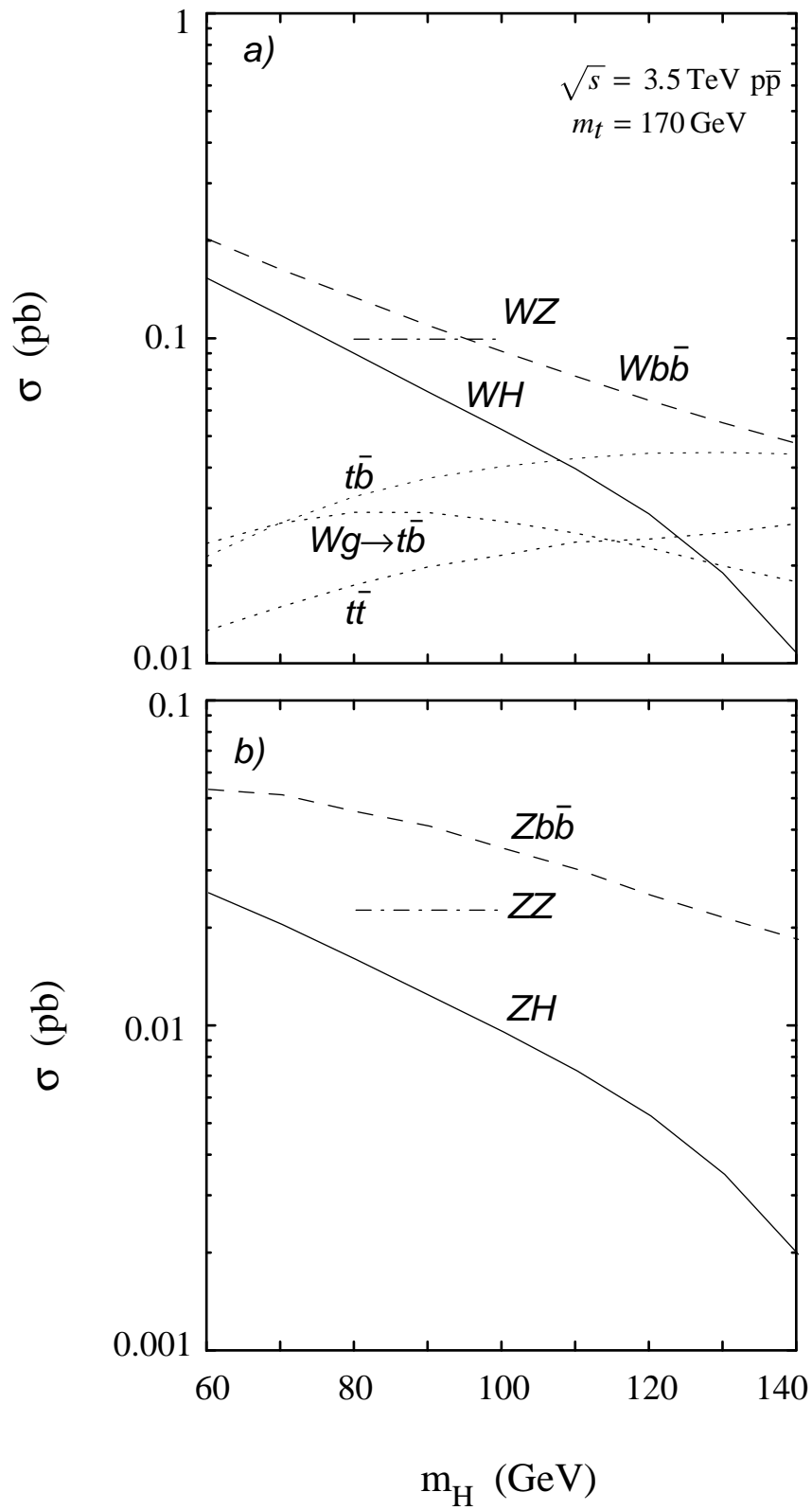


Figure 3

This figure "fig1-4.png" is available in "png" format from:

<http://arxiv.org/ps/hep-ph/9404247v2>



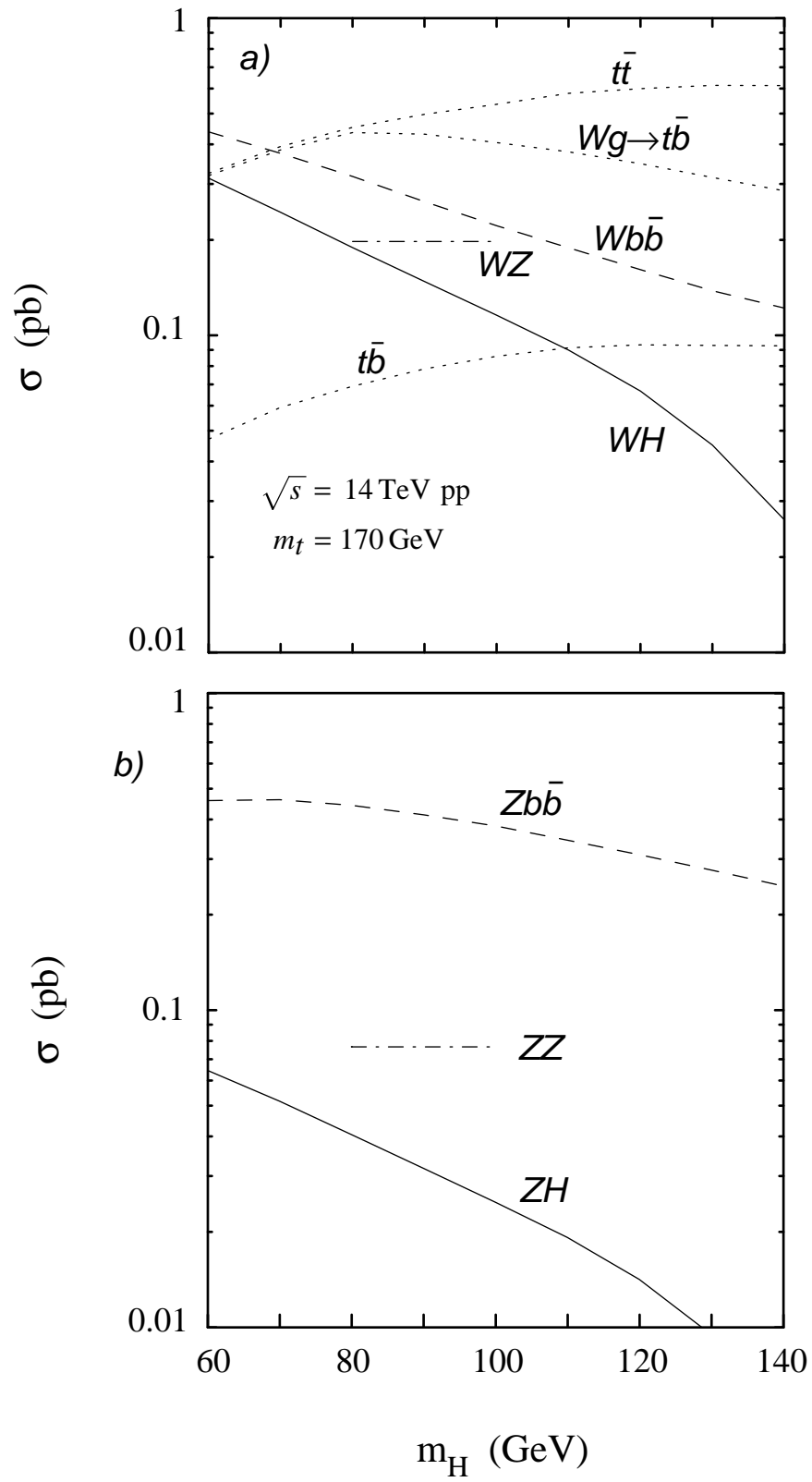


Figure 4

This figure "fig1-5.png" is available in "png" format from:

<http://arxiv.org/ps/hep-ph/9404247v2>

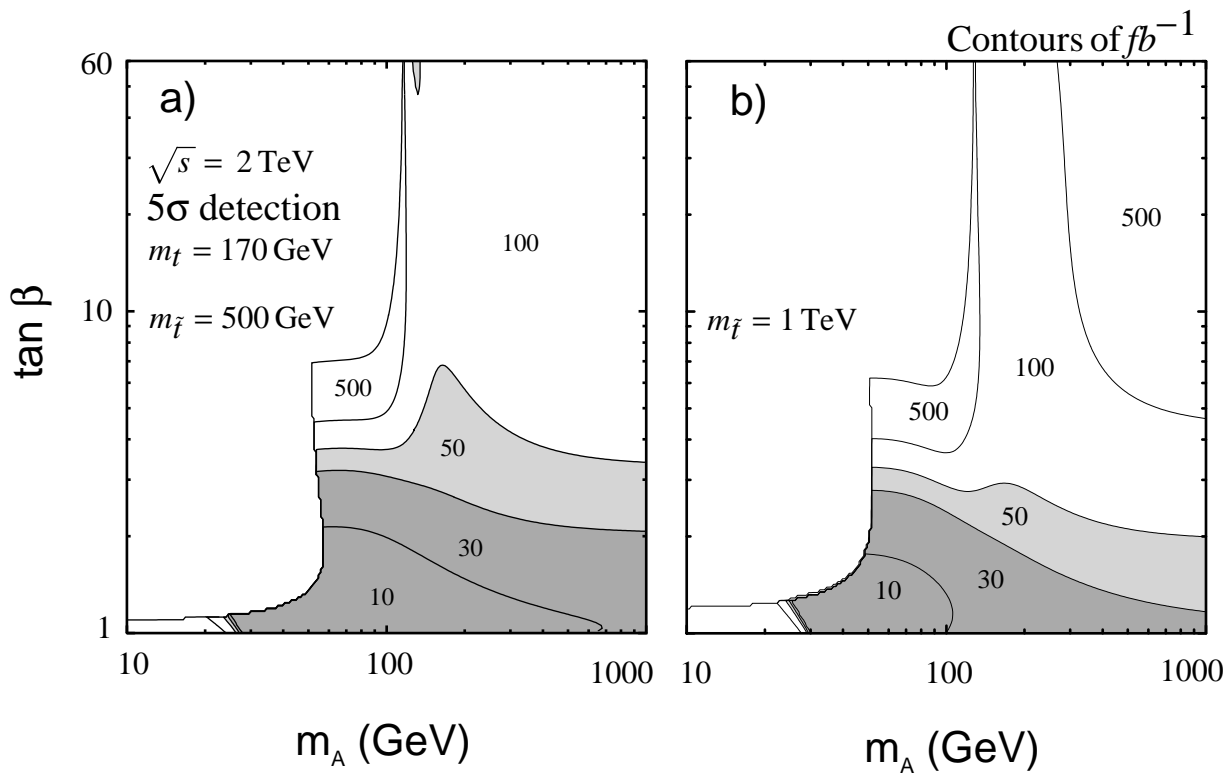


Figure 5

This figure "fig1-6.png" is available in "png" format from:

<http://arxiv.org/ps/hep-ph/9404247v2>

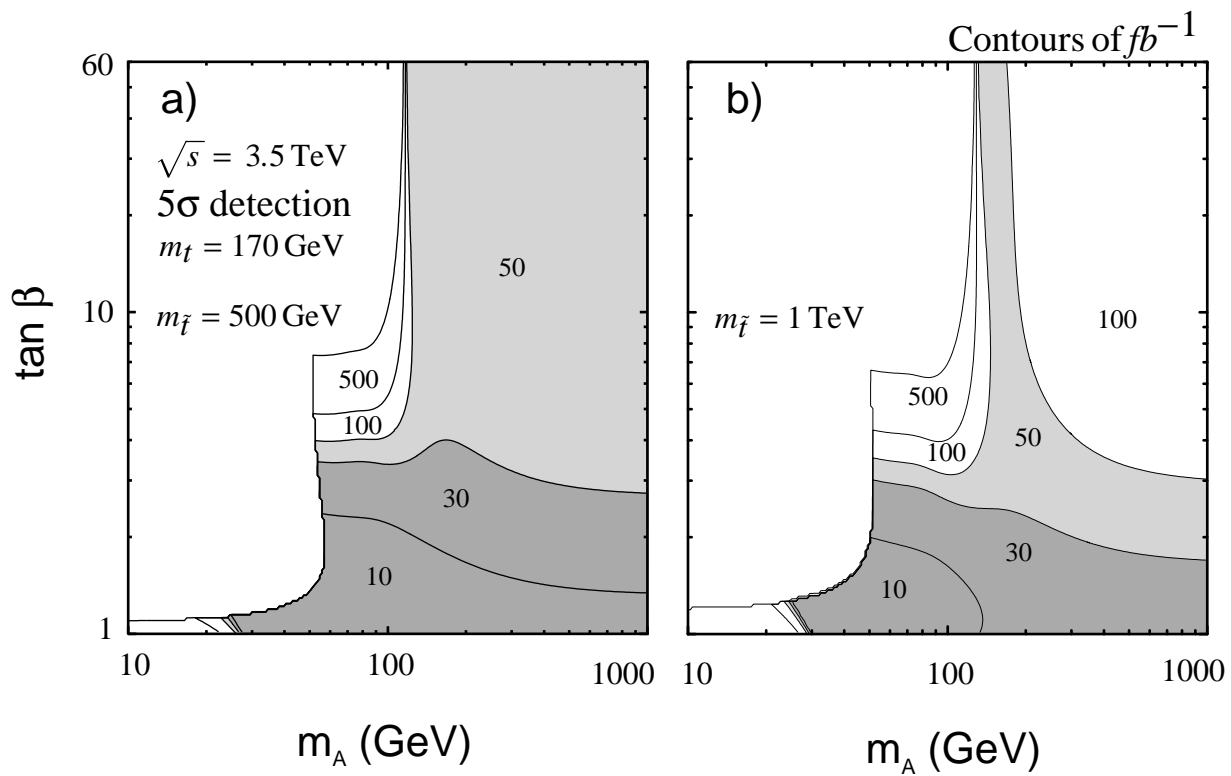


Figure 6

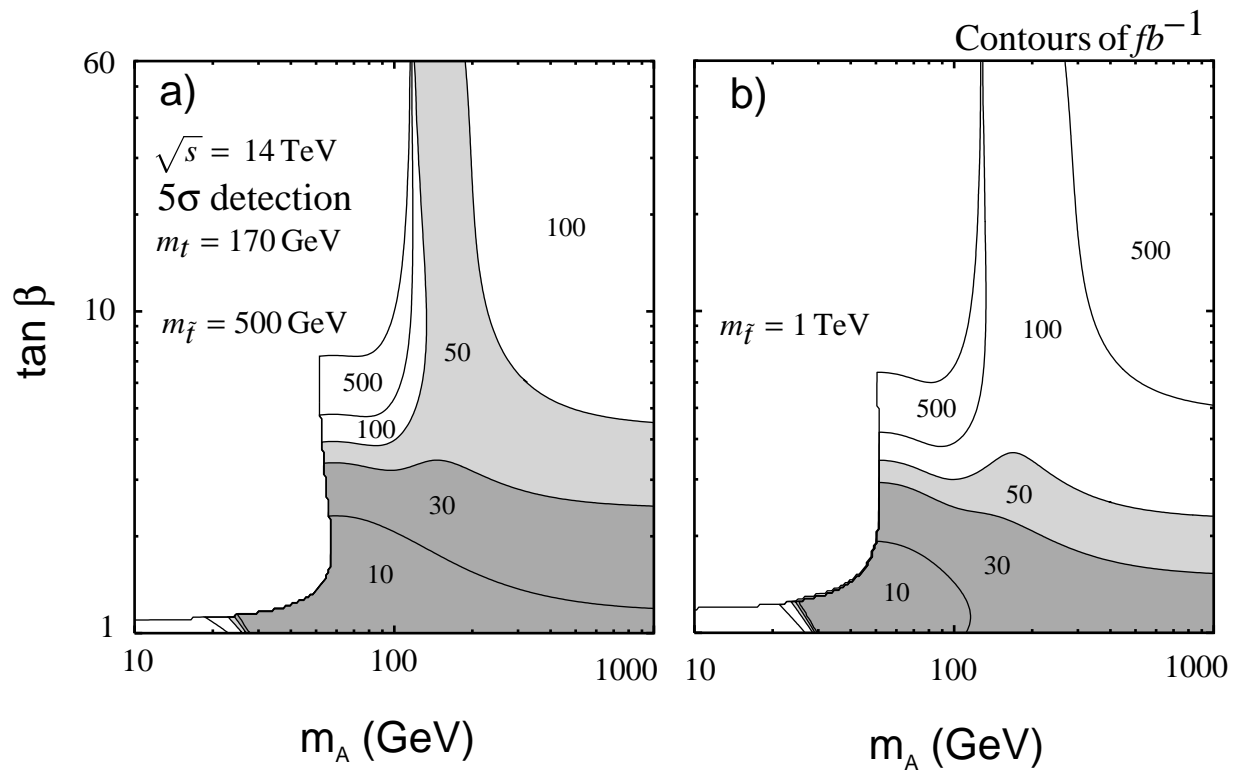


Figure 7